Optica Applicata, Vol. XLII, No. 2, 2012
DOI: 10.5277/oa120210

Preparation and photocatalytic activity of vanadium/silver doped TiO_2 thin films obtained by sol–gel method

MAREK NOCUŃ*, SŁAWOMIR KWAŚNY

AGH – University of Science and Technology, Department of Material Science and Ceramic, al. Mickiewicza 30, 30-059 Kraków, Poland

*Corresponding author: nocun@agh.edu.pl

In our investigation, V/Ag doped TiO_2 thin films were prepared on glass substrates. A thin film of SiO_2 was prepared as a blocking layer by the dip coating sol–gel technique. A catalytic effect was investigated for obtained samples using Rhodamine B as a probe. Transmittances of the samples were characterized using a UV–VIS spectrophotometer. Subsequently band-gap energy (E_g) was estimated for these films. Chemical composition of the samples was studied by photoelectron spectroscopy (XPS). Powders obtained from sols were characterized by FTIR spectroscopy and X-ray diffraction (XRD).

Keywords: sol–gel, V/Ag doped TiO_2, photocatalytic properties, structure.

1. Introduction

Titanium dioxide is one of the best-known photocatalysts and has been extensively investigated for the degradation of many organic compounds like organic pollutants [1, 2], volatile organic compounds [3], dyes [4–6], photo killing of bacteria [7], *etc*., TiO_2 is also utilized in glass technology as an active layer of self-cleaning glasses [8–12]. However, the application of TiO_2 is limited by its wide band-gap energy (3.2 eV for anatase), which requires ultraviolet irradiation ($\lambda \leq 387$ nm) to obtain the photocatalytic effect [13]. Hence, many researchers are working on the preparation of the photocatalyst with high photocatalytic activities in a visible light region or near visible at least. One way to shift absorption into a visible range is to dope TiO_2 with other materials as an optical response of any material is determined by its electronic structure, and this is closely related to its chemical composition [14]. The electronic structure of TiO_2 can be altered by doping it with different metals [14–17]. Recently, much interest has been directed towards the vanadia–titania system to extend the absorption threshold to a visible-light region for a better photocatalytic performance [18, 19]. Also the modification with Ag was reported to remarkably improve the catalyst performance [20].

In this study, a vanadium/silver system was chosen as a dopant for titanium sol. The physical, structural, and chemical properties of the V/Ag–TiO_2 samples were characterized by several techniques. Rhodamine B was used as a catalytic activity probe.

2. Experiment

2.1. Preparation of silica passivation layer

About a 100 nm thick film of silica was formed on a soda lime glass substrate as an alkali barrier. The sol solutions were prepared using tetraethyl orthosilicate (TEOS, Sigma-Aldrich). Ethanol 95% and 2-propanol (Polish Chemicals) were used as solvents. Hydrolysis reaction was catalyzed by 1 M HCl (Polish Chemicals). Chemical composition of the sols is shown in Tab. 1, while the preparation procedure in Fig. 1.

T a b l e 1. Chemical composition of the silica sol.

Symbol	TEOS [mol]	C_2H_5OH [mol]	H_2O [mol]	HCl [mol]	C_3H_8O [mol]
S	1	3	6	0.15	16.35

The glass substrate was ultrasonically washed in 20% acetic acid for 30 minutes, then ultrasonically washed in ethanol and distilled water for 15 minutes, and dried at room temperature. A thin film was prepared by the dip-coating technique using the speed of withdrawing of 6.6 cm/min. Samples were dried at room temperature and calcinated at 400 °C for 30 min. The thickness of the silica film was calculated from ellipsometric measurements using PHE 102 Angstrom Advance ellipsometer. In this way, a barrier layer for sodium in the form of a thin SiO_2 layer was obtained. The thickness of the layer was 90 nm.

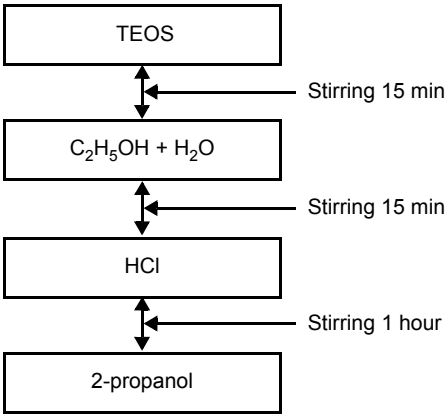

Fig. 1. Sol *S* preparation procedure.

2.2. Preparation of titania sol

Titania sol solution *T* was prepared using tetraethyl orthotitanate (TEOT, Sigma--Aldrich). 2-propanol (Polish Chemicals) was used as a solvent. Hydrolysis reaction

T a b l e 2. Chemical composition of the titania sol.

Symbol	TEOT [mol]	H_2O [mol]	HCl [mol]	C_3H_8O [mol]
T	1	4.75	0.28	118.3

was catalyzed by 1 M HCl (Polish Chemicals). Chemical composition of the sols is shown in Tab. 2, while the preparation procedure was the same as used in case of sol *S* preparation – Fig. 1.

2.3. Preparation of V/Ag solution

The solution of vanadium/silver and acetyl acetone was prepared in the following way: 0.5 g of V_2O_5 was mixed with 0.25 g of Ag_2CO_3, and 20 ml of H_2O_2 was added. The reaction of vanadium with water peroxide was highly exothermic and was carried out in water bath. Brown liquid with dark brown sediment was obtained as a result. The sediment was dried at 40 °C to remove water and dissolved in 10 ml of acetyl acetone. Marine colour solution was obtained as a result of vanadium/silver complex formation.

2.4. Formation of V/Ag doped TiO_2 thin film layer

50 ml of sol *T* was mixed with 2, 7, and 12 ml of the prepared V/Ag solution, receiving three sols with titania/vanadium/silver molar ratio: 1/0.026/0.0086, 1/0.092/0.03, and 1/0.16/0.05, respectively. The sols were stable over 2 months.

Thin films were deposited by the dip-coating technique using previously prepared SiO_2 coated microscope slides as a substrate. Samples were dried at room temperature and calcinated at 200, 300, 350 and 400 °C for 60 min.

2.5. Characterization of thin films and gels

Optical properties of the films were measured using a JASCO V-650 spectrophotometer. UV–VIS spectra were recorded from 300 to 1100 nm with 1 nm resolution.

The structure of a thin film is difficult to analyze due to its low thickness so we analyze the structure of relevant gel. In order to do this, sols were left to gelation at room temperature and next dried at 100 °C. The structure was studied using infrared spectroscopy. FTIR spectra were recorded with a Bruker Vertex 70V spectrometer. The spectra were collected in the mid infrared regions (4000–400 cm^{-1}) after

256 scans at 4 cm^{-1} resolution. Samples were prepared by the standard KBr pellets method.

Surface compositions of the samples were established from XPS measurements using a VSW spectrometer. Al Kα 200 W was used as an X-ray source. All spectra were calibrated with the binding energy of apparatus carbon C 1*s* peak E_b = 284.6 eV [20–22]. Curve fitting procedure was carried out using a XPSPEAK 4.1 program (Raymunda W.M. Kwok, The Chinese University of Hong Kong).

WAXS (wide angle X-ray scattering) was used for determination of a crystalline structure. The measurements were carried out on a Philips X'Pert Pro MD diffractometer. Cu Kα radiation was used as an X-ray source. Standard Bragg–Brentano geometry with *h*–2*h* setup was applied (0.008° step size and 5–90° 2 h range).

A differential thermal analysis of the sols was done using a Derivatograph Q-1500D. Samples were heated from 25 °C to 1000 °C at 10 °C/min in air environment.

3. Results and discussion

3.1. Optical properties

The transmittance of the glass samples with silica and titanium/vanadium/silver thin films is presented in Fig. 2. In a visible range, the transmittance is higher than 80% for all cases. An increase in vanadium/silver content leads to an increase in transmittance but this effect is not significant – Fig. 2**a**. The influence of annealing temperature on transmittance is also insignificant and higher annealing temperature gives higher transmittance – Fig. 2**b**.

In Figure 3 the changes in the refractive index with wavelength and annealing temperature in case of films prepared from sol *T* with 7 ml of V/Ag have been shown. The refractive index of the films with V/Ag addition is much lower in the visible range than the refractive index of the film prepared from titanium sol. It is most probably

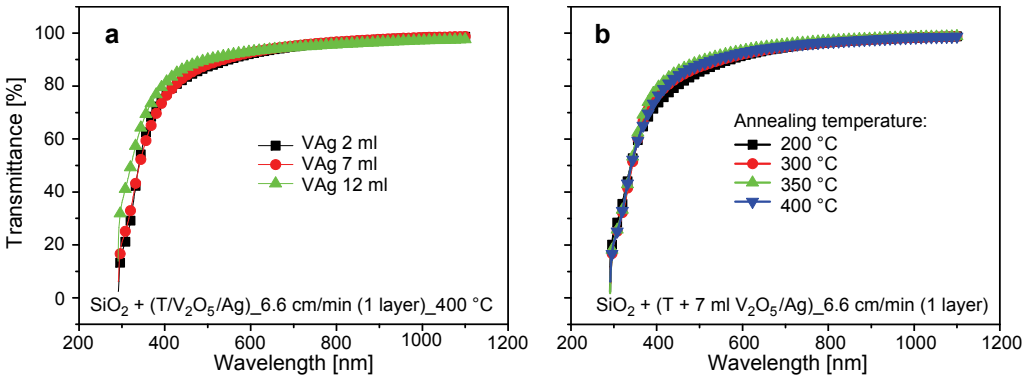

Fig. 2. Transmittance spectra of the samples with two layers (both sides of glass were covered) of a thin film: samples with different amount of vanadium/silver content annealed at 400 °C during 1 h (**a**), transmittance changes with annealing temperature for samples having 7 ml of vanadium/silver content (**b**).

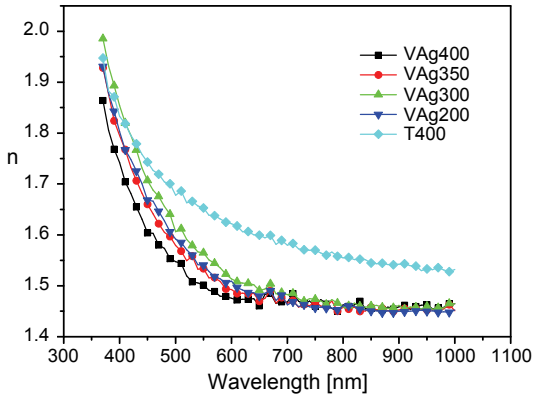

Fig. 3. Changes in the refractive index of the film based on the sol with 7 ml of V/Ag with annealing temperature.

due to a complexing ability of acetyl acetone, which leads to films with higher porosity. Annealing temperature does not influence much the refractive index, however the refractive index is decreasing with increasing temperature. Higher annealing temperature produces denser films with lower porosity, due to sintering.

Optical band gaps of V/Ag doped TiO_2 films ware calculated from ellipsometry spectra and the results are presented in Fig. 4. In a direct band gap semiconductor, $\alpha(E_n)$ is expressed by the following equation:

$$\alpha(E_n) = A(E_n - E_g)^{1/2}$$

where: α – absorption coefficient, E_n – photon energy, E_g – band gap energy, A – proportional constant. Plotting $\alpha^2 E_n^2$ versus E_n, E_g can be determined from the interception of a straight asymptote line with a horizontal axis.

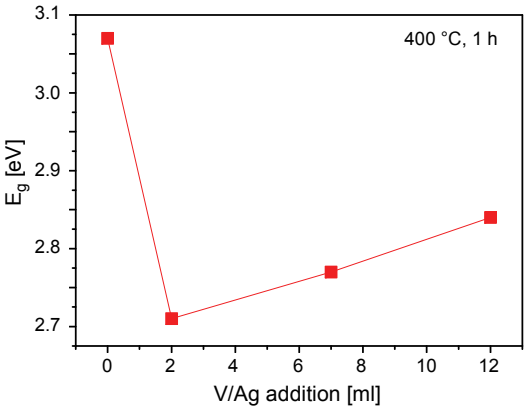

Fig. 4. Changes in the optical band gap with vanadium and silver content for different annealing temperatures estimated from ellipsometry measurements. Line is drawn to show the tendency.

The calculated value of the energy band gap ranges from 3.07 to 2.71 eV. The lowest value (2.71 eV) was measured for the sample with 2 ml of V/Ag annealed at 400 °C – Fig. 4. Generally, a further increase in V/Ag content leads to a slight increase in the optical energy band gap. The highest decrease in the energy band gap, from 3.07 to 2.71 eV, is seen for the samples with 2 ml of V/Ag. The band gap of 2.71 eV should give a possibility to induce the photocatalytic effect by a near UV light, as it corresponds to 458 nm.

3.2. FTIR results

FTIR results of gels with different amount of vanadium/silver are shown in Figure 5.

A broad absorption peak at 3100–3800 cm^{-1} wavelength range is assigned to the stretching modes of O–H bonds and related to free water (capillary pore water and surface absorbed water). The peaks related to $–CH_3$ and $–CH_2–$ groups are observed around 1360, 1526, 1582, 2923 and 2970 cm^{-1} [21, 22]. In the range between 400–1000 cm^{-1}, where Ti–O bond vibrations occur, some differences are noticed with an increase in vanadium content, which could be assigned to the presence of vanadium in different valence states in the TiO_2 lattice [23]. The bands at 1340–1378 cm^{-1} in the spectra of low vanadia can be assigned to the anatase phase [24]. The anatase and rutile phases of titania exhibit also strong absorption bands in the region of 850–650 and 800–650 cm^{-1}, respectively [25].

Although the band at 1022 cm^{-1} is assigned to the V=O stretching vibration [6–8], the one in the vicinity of 819 cm^{-1} is attributable to the coupled vibration between

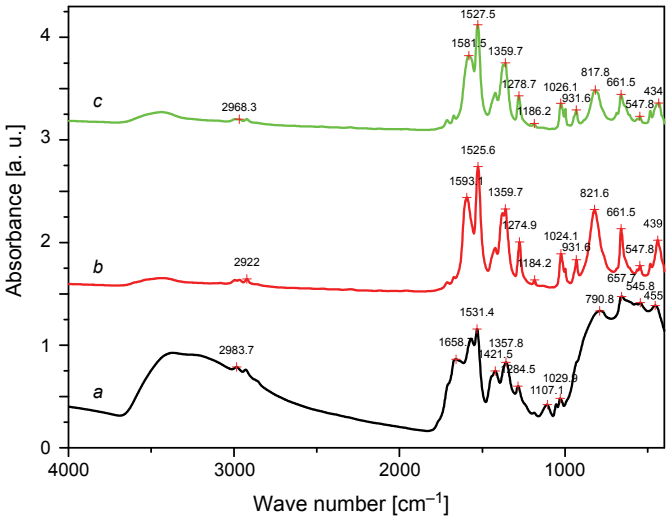

Fig. 5. FTIR spectra of the powders sol *T* with addition of: 2 ml of V/Ag (*a*), 7 ml of V/Ag (*b*), and 12 ml of V/Ag (*c*).

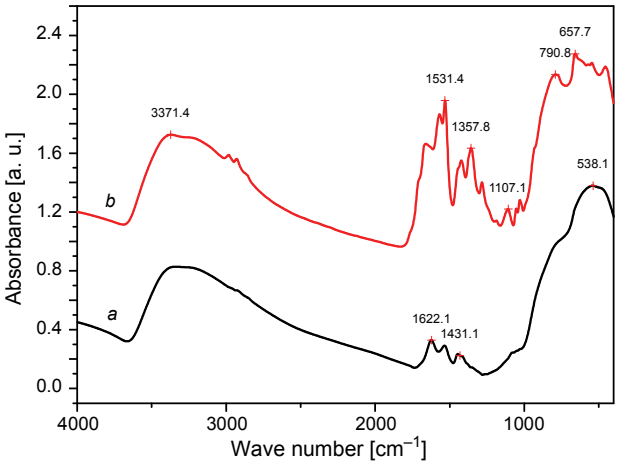

Fig. 6. FTIR spectra of the powders: *T* sol (*a*) and *T* with 2 ml of V/Ag (*b*).

V=O and to V–O–V [26]. Generally, the IR band of V=O in crystalline V_2O_5 appeared at 1020–1025 cm^{-1} and the Raman band at 995 cm^{-1} [26–28].

The band at 1010–1039 cm^{-1}, commonly occurring in the spectra of the fresh V_2O_5 catalysts, should be ascribed to the stretching frequency of VO_x units and VO_x clusters [24]. The bands at 994 and 940 cm^{-1} can be attributed to surface VO_x species [24].

Absorption bands in the range of 1585–1278 cm^{-1} are connected with acetyl acetone (AcAc) present in the gel structure. It is clearly seen comparing the IR spectrum of gel *T* without AcAc and the one of the gel with AcAc – Fig. 6. Sols with AcAc are much more stable than the sols without AcAc. It can be explained by a complexing ability of AcAc which prevents aggregation of TiO_2.

3.3. Photoelectron spectroscopy XPS

XPS analyzes are carried out to confirm the presence of vanadium and silver in the films as well as to determine their chemical state. The results are presented in Figs. 7 to 10.

Oxygen O 1*s* regions consist of two peaks, what is shown in Fig. 7. Oxygen with binding energy 529.5 eV is associated with titanium. Such value of binding energy was also published for V_2O_5 compound [29]. Each O 1*s* spectrum is fitted to two separate peaks with binding energy 529.5 and 532.1 eV seen in the inset in Fig. 7. The peaks are assigned to the lattice oxygen (Ti–O–Ti) and chemisorbed oxygen (–OH), respectively [30]. Oxygen O–(Ti) 1*s* binding energy shifts into higher value with V/Ag concentration and reaches 529.7 eV for 12 ml V/Ag. This change can be connected with V_2O_5 formation as a separate phase. Titanium Ti 2*p* region contains only one peak with binding energy 458.25 eV (Ti $2p_{3/2}$) so only one surrounding

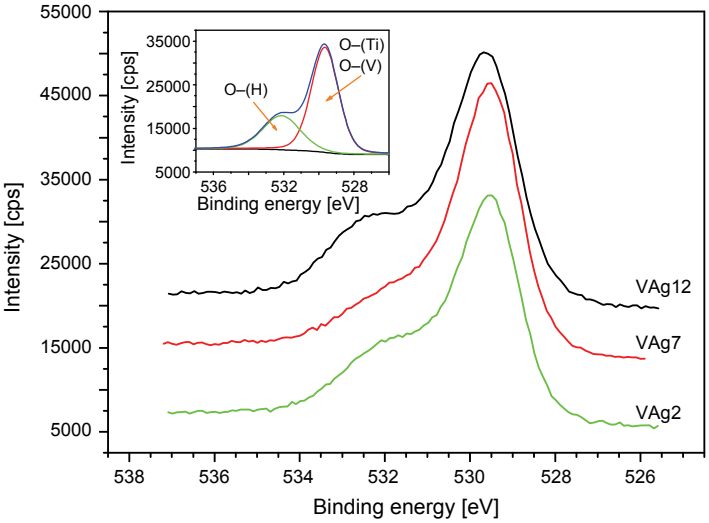

Fig. 7. High resolution XPS spectra of oxygen O 1*s* region.

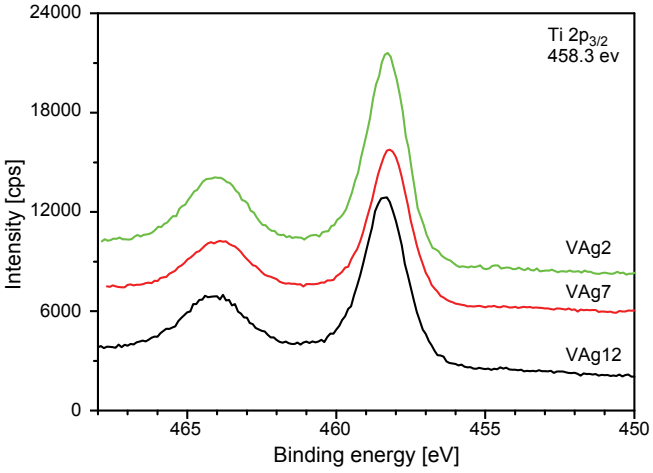

Fig. 8. High resolution XPS spectra of Ti 2*p* region.

arrangement of titanium is expected – Fig. 8. This value of binding energy is characteristic of TiO_2 [31].

XPS spectra of V 2*p* region are dominated by oxygen satellite peaks as the concentration of vanadium is very low, however it is possible to distinguish V 2*p* peak – Figure 9.

The binding energy of V $2p_{3/2}$ peak is 515.8 eV, usually reported for VO_2 [32]. One can accept that vanadium is present in the structure as V^{4+}. If so, vanadium can substitute titanium in the structure as ionic radii of both ions are similar. The amount

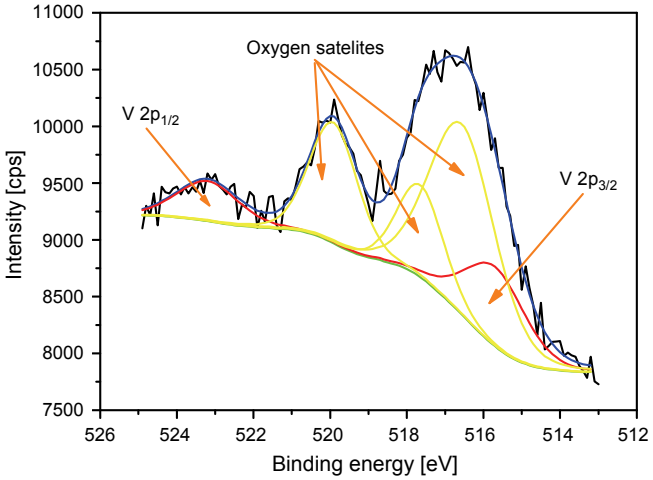

Fig. 9. High resolution XPS spectra of V 2*p* region. Thin film with 12 ml of V/Ag.

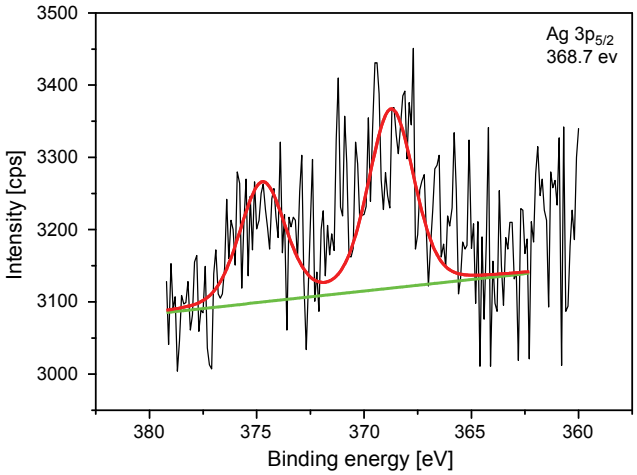

Fig. 10. High resolution spectra of Ag 3*d* detected in the sample with 12 ml of V/Ag.

of silver in the samples with 2 and 7 ml of V/Ag was under detection limit and even in the sample with 12 ml of V/Ag was merely detected – Fig. 10. The binding energy of silver was established to be 368.7 eV and is characteristic of the ionic form (most probably Ag^{1+}) of silver as silver in a metallic state has 1 eV lower binding energy [32].

3.4. X-ray diffraction

The effect of calcination temperature on sample crystallinity was investigated by X-ray diffraction – Fig. 11. The XRD pattern of the V/Ag–Ti samples after calcination at 350 °C displays only anatase reflections – curve *a*. Gel after calcination at 450 °C

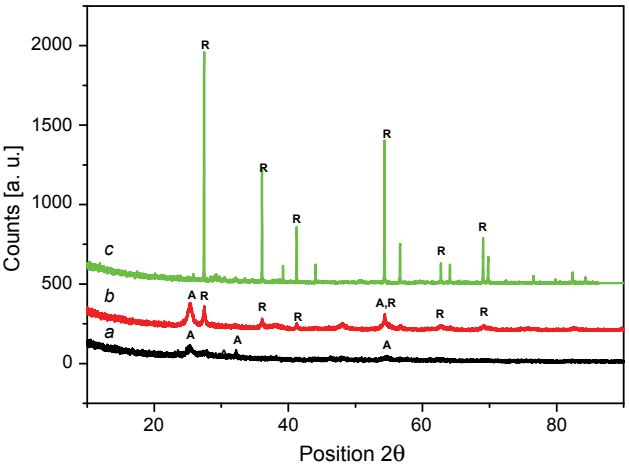

Fig. 11. X-ray powder diffraction patterns of *T* 7 ml of V/Ag/gel calcinated at: 350 °C (*a*), 450 °C (*b*) and 950 °C (*c*).

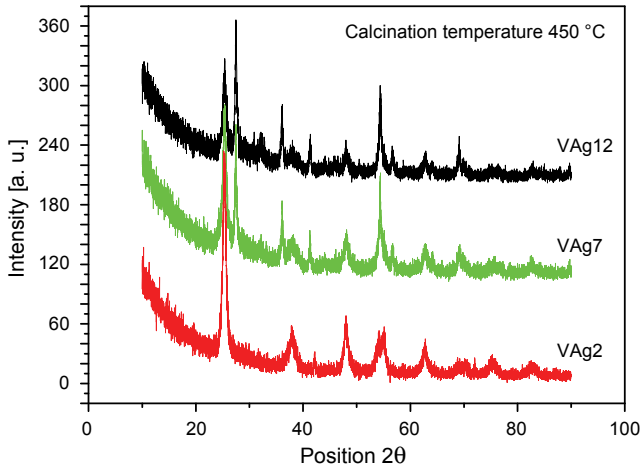

Fig. 12. X-ray powder diffraction patterns of the samples calcinated at 450 °C.

consists of two phases: anatase 75% and rutile (25%) – curve *b*. The higher the calcination temperature, the more percentage of rutile phase is observed. At 900 °C the only phase detected is rutile as a phase transition undergoes from anatase to rutile [33]. In Figure 12 the changes in the phase composition versus the vanadium silver content are shown. Samples were calcinated at 450 °C. The sample with 2 ml of V/Ag contains only anatase, while the samples with 7 and 12 ml of V/Ag consist of anatase and rutile. These results imply that V/Ag doping promotes the anatase to rutile phase transformation and this transformation undergoes at much lower temperature than it is observed in case of polycrystalline anatase (usually above 900 °C).

3.5. Photocatalytic activity

The photocatalytic activity of a thin film was evaluated on the basis of changes in the Rhodamine B peak area before and after UV/VIS exposure. Absorption spectra were measured with a spectrometer. Rhodamine B solution was prepared by dissolving 0.6 g Rhodamine in 100 ml of ethanol. Samples were coated by Rhodamine solution using the dip-coating technique. A uniform and homogeneous layer of a dye was obtained. The dye-coated samples were irradiated with a UV fluorescent lamp 18 W or halogen lamp in case of testing photocatalitic activity in a visible range. The photocatalytic activity is presented as a decrease in the Rhodamine peak area expressed in %:

$$\text{Pha} = \frac{R_a - R_b}{R_a} \times 100$$

where: Pha – photocatalytic activity, R_b – Rhodamine peak area before exposure, R_a – Rhodamine peak area after exposure.

The surface area of the absorption peak of Rhodamine decreases after UV radiation by 20% in case of all samples modified by vanadium and silver, but in the sample with 2 ml of V/Ag (400 °C) the decrease was by 42% – Fig. 13**a**. In the same condition, Pha of the sample prepared from pure titanium sol was only 12% and above 20% when the sample was calcinated at 400 °C. High photocatalytic activity of the sample with 2 ml of V/Ag results from a high content of the anatase phase. A higher V/Ag content leads to the transformation of anatase into rutile and the decrease in Pha. In case of VIS, the radiation activity of the sample with titanium layer was ~10%. The activity of the samples with vanadium and silver strongly depends on annealing temperature and V/Ag content. Generally, an increase in annealing temperature up to 300 °C increases the activity, but further increase leads to decreasing activity – Fig. 13**b**. It is because the relation between anatase and rutile changes into rutile formation,

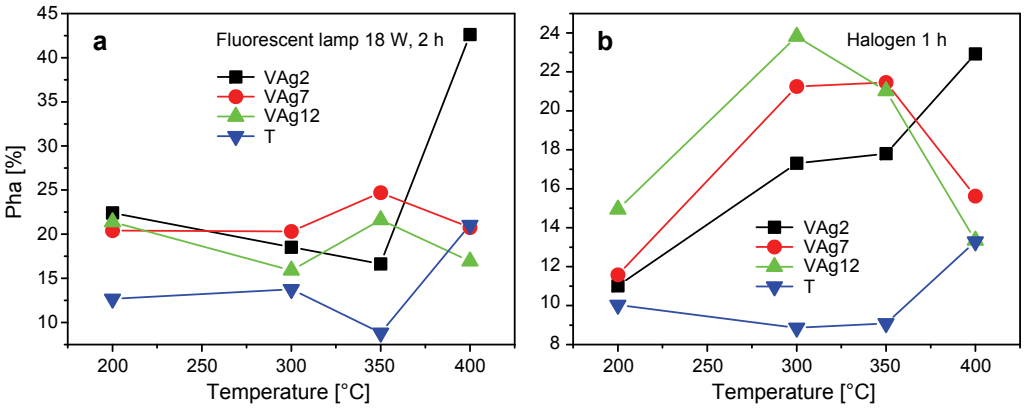

Fig. 13. Photocatalytic activity versus temperature; under fluorescence illumination (**a**), under visible light radiation (**b**).

however phase transformation does not happen in case of sample with 2 ml of V/Ag so the activity of this sample is rising with temperature reaching 23% – Fig. 13**b**.

4. Conclusions

An addition of vanadium and silver increases photoactivity of titania film in UV as compared to pure titania. The most effective sol composition is 1:0.026:0.0086 molar ratio of Ti:V:Ag. Vanadium and silver increase also the activity of Ti film in a visible range. In this case, the most effective molar ratio of Ti:V:Ag sol is 1:0.16:0.05 and optimum annealing temperature is 300 °C.

Acknowledgements – The present work was financially supported by the Polish Ministry of Science and Higher Education, grant No. 11.11.160.365.

References

[1] PRAIRIE M.R., EVANS L.R., STANGE B.M., MARLINEZ S.L., *An investigation of titanium dioxide photocatalysis for the treatment of water contaminated with metals and organic chemicals*, Environmental Science and Technology **27**(9), 1993, pp. 1776–1782.

[2] PATSOURA A., KONDARIDES D.I., VERYKIOS X.E., *Photocatalytic degradation of organic pollutants with simultaneous production of hydrogen*, Catalysis Today **124**(3–4), 2007, pp. 94–102.

[3] ZOU L., LUO Y., HOOPER M., HU E., *Removal of VOCs by photocatalysis process using adsorption enhanced TiO_2–SiO_2 catalyst*, Chemical Engineering and Processing: Process Intensification **45**(11), 2006, pp. 959–964.

[4] DOUSHITA K., KAWAHARA T., *Evaluation of photocatalytic activity by dye decomposition*, Journal of Sol-Gel Science and Technology **22**(1–2), 2001, pp. 91–98.

[5] SHOURONG ZHENG, JIANZHONG ZHENG, ZHIGANG ZOU, *Photo-catalytic properties of TiO_2 supported layered compounds for dye removal*, Research on Chemical Intermediates **31**(4–6), 2005, pp. 493–498.

[6] FENG CHEN, JINCAI ZHAO, HISAO HIDAKA, *Highly selective deethylation of rhodamine B: Adsorption and photooxidation pathways of the dye on the TiO_2/SiO_2 composite photocatalyst*, International Journal of Photoenergy **5**(4), 2003, pp. 209–217.

[7] SUNADA K., WATANABE T., HASHIMOTO K., *Studies on photokilling of bacteria on TiO_2 thin film*, Journal of Photochemistry and Photobiology A: Chemistry **156**(1–3), 2003, pp. 227–233.

[8] AEGERTER M.A., ALMEIDA R., SOUTAR A., TADANAGA K., YANG H., WATANABE T., *Coatings made by sol–gel and chemical nanotechnology*, Journal of Sol-Gel Science and Technology **47**(2), 2008, pp. 203–236.

[9] KOMINAMI H., TAKADA Y., YAMAGIWA H., KERA Y., INOUE M., INUI T., *Synthesis of thermally stable nanocrystalline anatase by high-temperature hydrolysis of titanium alkoxide with water dissolved in organic solvent from gas phase*, Journal of Materials Science Letters **15**(3), 1996, pp. 197–200.

[10] SOPYAN I., WATANABE M., MURASAWA S., HASHIMOTO K., FUJISHIMA A., *An efficient TiO_2 thin-film photocatalyst: photocatalytic properties in gas-phase acetaldehyde degradation*, Journal of Photochemistry and Photobiology A: Chemistry **98**(1–2), 1996, pp. 79–86.

[11] DONG HYUN KIM, ANDERSON M.A., *Solution factors affecting the photocatalytic and photoelectrocatalytic degradation of formic acid using supported TiO_2 thin films*, Journal of Photochemistry and Photobiology A: Chemistry **94**(2–3), 1996, pp. 221–229.

[12] PERAL J., OLLIS D.F., *Heterogeneous photocatalytic oxidation of gas-phase organics for air purification: Acetone, 1-butanol, butyraldehyde, formaldehyde, and m-xylene oxidation*, Journal of Catalysis **136**(2), 1992, pp. 554–565.

[13] LINSEBIGLER A.L., GUANGQUAN LU, YATES J.T., *Photocatalysis on TiO_2 surfaces: Principles, mechanisms, and selected results*, Chemical Reviews **95**(3), 1995, pp. 735–758.

[14] XIAOBO CHEN, MAO S.S., *Titanium dioxide nanomaterials: Synthesis, properties, modifications, and applications*, Chemical Reviews **107**(7), 2007, pp. 2891–2959.

[15] RAMPAUL A., PARKIN I.P., O'NEILL S.A., DESOUZA J., MILLS A., ELLIOTT N., *Titania and tungsten doped titania thin films on glass; active photocatalysts*, Polyhedron **22**(1), 2003, pp. 35–44.

[16] KEMP T.J., MCINTYRE R.A., *Transition metal-doped titanium(IV) dioxide: Characterisation and influence on photodegradation of poly(vinyl chloride)*, Polymer Degradation and Stability **91**(1), 2006, pp. 165–194.

[17] YANFANG SHEN, TIANYING XIONG, HAO DU, HUAZI JIN, JIANKU SHANG, KE YANG, *Phosphorous, nitrogen, and molybdenum ternary co-doped TiO2: preparation and photocatalytic activities under visible light*, Journal of Sol-Gel Science and Technology **50**(1), 2009, pp. 98–102.

[18] SONG LIU, TIANHUA XIE, ZHI CHEN, JIANTAO WU, *Highly active V–TiO_2 for photocatalytic degradation of methyl orange*, Applied Surface Science **255**(20), 2009, pp. 8587–8592.

[19] WU J. C.-S., CHEN CH.-H., *A visible-light response vanadium-doped titania nanocatalyst by sol–gel method*, Journal of Photochemistry and Photobiology A: Chemistry **163**(3), 2004, pp. 509–515.

[20] HAO GE, GUANGWEN CHEN, QUAN YUAN, HENGQIANG LI, *Gas phase partial oxidation of toluene over modified V_2O_5/TiO_2 catalysts in a microreactor*, Chemical Engineering Journal **127**(1–3), 2007, pp. 39–46.

[21] JIAGUO YU, YU J.C., XIUJIAN ZHAO, *The effect of SiO_2 addition on the grain size and photocatalytic activity of TiO_2 thin films*, Journal of Sol-Gel Science and Technology **24**(2), 2002, pp. 95–103.

[22] GUNZLER H., GREMLICH H.U., [Eds.], *IR Spectroscopy. An Introduction*, Wiley-VCH, 2002, p. 208.

[23] CRISAN M., ZAHARESCU M., CRISAN D., ION R., MANOLACHE M., *Vanadium doped sol–gel TiO_2 coatings*, Journal of Sol-Gel Science and Technology **13**(1–3), 1998, pp. 775–778.

[24] NARAYANA K.V., VENUGOPAL A., RAMA RAO K.S., KHAJA MASTHAN S., VENKAT RAO V., KANTA RAO P., *Ammoxidation of 3-picoline over V_2O_5/TiO_2 (anatase) system. II. Characterisation of the catalysts by DTA, SEM, FTIR, ESR and oxygen and ammonia chemisorption*, Applied Catalysis A: General **167**(1), 1998, pp. 11–22.

[25] REDDY B.M., GANESH I., KHAN A., *Preparation and characterization of In_2O_3–TiO_2 and V_2O_5/In_2O_3–TiO_2 composite oxides for catalytic applications*, Applied Catalysis A: General **248**(1–2), 2003, pp. 169–180.

[26] KWON S.H., SEO K.C., PAE Y.I., SOHN J.R., *Spectroscopic study of V_2O_5 supported on ZrO_2 and modified with MoO_3*, Theories and Applications of Chemical Engineering **8**(2), 2002, pp. 2633–2636.

[27] JONG RACK SOHN, MAN HO LEE, IM JA DOH, YOUNG IL PAE, *Solid-state ^{51}V NMR and infrared spectroscopic study of vanadium oxide supported on ZrO_2–WO_3*, Bulletin of the Korean Chemical Society **19**(8), 1998, pp. 856–862.

[28] JONG RACK SOHN, CHEUL KYU LEE, *Effect of V_2O_5 modification in V_2O_5/TiO_2–ZrO_2 catalysts on their surface properties and catalytic activities for acid catalysis*, Bulletin of the Korean Chemical Society **28**(12), 2007, pp. 2459–2465.

[29] NEFEDOV V.I., GATI D., DZHURINSKII B.F., SERGUSHIN N.P., SALYN YA.V., *Simple and coordination compounds*, Russian Journal of Inorganic Chemistry **20**, 1975, pp. 2307–2314.

[30] WENFANG ZHOU, QINGJU LIU, ZHONGQI ZHU, JI ZHANG, *Preparation and properties of vanadium--doped TiO_2 photocatalysts*, Journal of Physics D: Applied Physics **43**(3), 2010, article 035301.

[31] HYUNG-JOO CHOI, JUN-SIK KIM, MISOOK KANG, *Photodecomposition of concentrated ammonia over nanometer-sized TiO_2, V–TiO_2, and Pt/V–TiO_2 photocatalysts*, Bulletin of the Korean Chemical Society **28**(4), 2007, pp. 581–588.

[32] WAGNER C.D., MOULDER J.F., DAVIS L.E., RIGGS W.M., *Handbook of X-Ray Photoelectron Spectroscopy*, Perking-Elmer Corporation, Physical Electronics Division, 1978.
[33] BRACONNIER B., PÁEZ C.A., LAMBERT S., ALIÉ CH., HENRIST C., POELMAN D., PIRARD J.P., CLOOTS R., HEINRICHS B., *Ag- and SiO_2-doped porous TiO_2 with enhanced thermal stability*, Microporous and Mesoporous Materials **122**(1–3), 2009, pp. 247–254.

Received September 30, 2011